
Some improvements of Xfem for cracked domains

E. Chahine ¹, P. Laborde², J. Pommier¹, Y. Renard³ and M. Salaün⁴

⁽¹⁾ INSA Toulouse, laboratoire MIP, CNRS UMR 5640, Complexe scientifique de Rangueil, 31077 Toulouse, France.

⁽²⁾ Université P. Sabatier, laboratoire MIP, CNRS UMR 5640, 118 route de Narbonne, 31062 Toulouse cedex 4, France.

⁽³⁾ INSA Lyon, Institut Camille Jordan, CNRS UMR 5208, 20, rue Albert Einstein, 69621 Villeurbanne, France.

⁽⁴⁾ ENSICA, 1 pl. Émile Blouin, 31056 Toulouse cedex 5, France.

Summary. The XFEM method for fracture mechanics is revisited. A first improvement is considered using an enlarged fixed enriched subdomain around the crack tip and a bonding condition for the corresponding degrees of freedom. An efficient numerical integration rule is introduced for the nonsmooth enrichment functions. The lack of accuracy due to the transition layer between the enrichment area and the rest of the domain leads to consider a pointwise matching condition at the boundary of the subdomain. An optimal rate of convergence is then obtained, numerically and theoretically, even for high degree polynomial approximation.

Key words: Fracture, finite elements, XFEM, optimal rate of convergence.

1 Introduction

In many industrial situations, it is of great interest to compute the advance of a crack for a two-dimensional domain (plate, shell) or a three-dimensional body. In 1999, Moës, Dolbow and Belytschko introduced in [9] a new methodology, the so-called Xfem method, which allows to make computations in a cracked domain, the crack growth being described independently of the mesh. This is an important advantage compared to existing methods where a remeshing step and an interpolation step are necessary each time an extension of the crack is computed, which can be sources of instabilities. Our goal is to evaluate the Xfem method in terms of efficiency and quality of approximation and, as far as it is possible, to give mathematical justifications to its efficiency. We also propose some improvements for some limitations of the method.

2 Model Problem

A linear elastic two-dimensional problem is considered on a cracked domain Ω (see Fig. 1), with an isotropic homogeneous material. On the boundary of the non-cracked domain $\overline{\Omega}$, a Dirichlet condition is applied on Γ_D and a Neumann condition is prescribed on Γ_N . The crack is denoted by Γ_C such that Γ_D , Γ_N and Γ_C form a partition of $\partial\Omega$.

The space of admissible displacements is

$$\mathcal{V} = \{v \in H^1(\Omega; \mathbb{R}^2); v = 0 \text{ on } \Gamma_D\},$$

and the equilibrium problem is written as follows:

$$\text{find } u \in \mathcal{V} \text{ s.t. } a(u, v) = l(v) \quad \forall v \in \mathcal{V},$$

where

$$a(u, v) = \int_{\Omega} \sigma(u) : \varepsilon(v) \, dx, \quad l(v) = \int_{\Omega} f \cdot v \, dx + \int_{\Gamma_N} g \cdot v \, d\Gamma,$$

and $\sigma(u) = \lambda \text{tr } \varepsilon(u) I + 2\mu \varepsilon(u)$ is the stress tensor, $\varepsilon(u)$ the linearized strain tensor, $\lambda > 0$ and $\mu > 0$ the Lamé coefficients, f and g some given force densities on Ω and Γ_N respectively. A traction free condition on the crack is assumed.

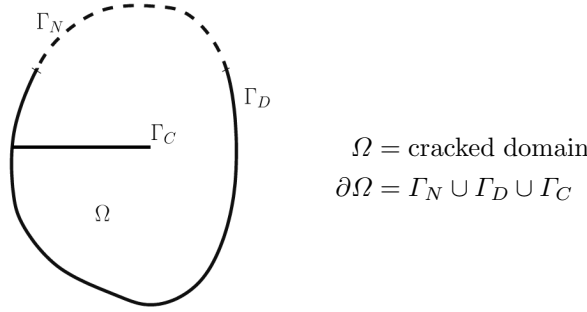


Fig. 1. A cracked domain.

The asymptotic displacement at the crack tip for the two opening modes u_I, u_{II} are given in polar coordinates (see Fig. 2) relatively to the crack tip by

$$u_I = \frac{K_I}{E} \sqrt{\frac{r}{2\pi}} \begin{pmatrix} \cos \frac{\theta}{2} \\ \sin \frac{\theta}{2} \end{pmatrix} (a + b \cos \theta)$$

$$u_{II} = \frac{K_{II}}{E} \sqrt{\frac{r}{2\pi}} (1 + \nu) \begin{pmatrix} \sin \frac{\theta}{2} (c + 2 + \cos \theta) \\ \cos \frac{\theta}{2} (2 - c - \cos \theta) \end{pmatrix},$$

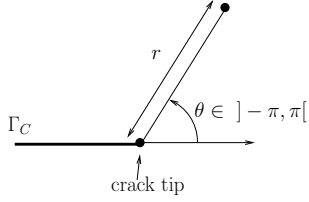


Fig. 2. Polar coordinates relatively to the crack tip.

where K_I and K_{II} are the stress intensity factors (see [8] for instance), and

$$a = 2 + \frac{2\mu}{\lambda + 2\mu}, \quad b = -2 \frac{\lambda + \mu}{\lambda + 2\mu}, \quad c = \frac{\lambda + 3\mu}{\lambda + \mu}.$$

The functions u_I and u_{II} belong to $H^{3/2-\varepsilon}(\Omega; \mathbb{R}^2)$ for any $\varepsilon > 0$ (see [6], chapter 4).

3 The classical Xfem

Let X^h be a scalar finite element space on a triangular mesh of the uncracked domain $\overline{\Omega}$. For instance, X^h will represent a P_k finite element method. Let also Y^h be a P_1 finite element space on the same mesh. We will denote by φ_i the basis functions (shape functions) of X^h and by ψ_i the ones of Y^h . The classical Xfem method is then characterized by the three following techniques.

- A representation of the discontinuity of the displacement across the crack with the enrichment

$$\sum_{i \in I_H} b_i H \varphi_i,$$

(in fact $\sum_{i \in I_H} b_i H \psi_i$ was proposed in original Xfem), where $H(x)$ is the step function being equal to $+1$ on one side of the crack and -1 on the other side. The set I_H corresponds to the basis functions whose support is completely cut by the crack (see [9]). One remarks that the discontinuity is not represented on the element containing the crack tip.

- The enrichment with the asymptotic displacement at the crack tip

$$\sum_{i \in I_F} \sum_{j=1}^4 c_{ij} F_j \psi_i,$$

where

$$F_1 = \sqrt{r} \sin \frac{\theta}{2}, \quad F_2 = \sqrt{r} \cos \frac{\theta}{2}, \quad F_3 = \sqrt{r} \sin \frac{\theta}{2} \cos \theta, \quad F_4 = \sqrt{r} \cos \frac{\theta}{2} \cos \theta,$$

and I_F is the set of basis functions whose support contains the crack tip (see [9] and Fig. 3). The singular function F_1 represents also the discontinuity on the element containing the crack tip.

- The approximation of the geometry of the crack by two level sets of functions ξ_h, ζ_h defined on a scalar fem (classically Y^h) allowing to define: $H(x) = \text{sign}(\xi_h(x)), r = \sqrt{\xi_h^2 + \zeta_h^2}$, and $\theta = \arctan \frac{\xi_h}{\zeta_h}$ (see [14]).

Consequently, the finite element space approximating the displacement on the cracked domain is defined as follows:

$$\mathcal{V}^h = \left\{ v^h = \sum_i a_i \varphi_i + \sum_{i \in I_H} b_i H \varphi_i + \sum_{i \in I_F} \sum_{j=1}^4 c_{ij} F_j \psi_i : a_i, b_i, c_{ij} \in \mathbb{R}^2 \right\} \quad (1)$$

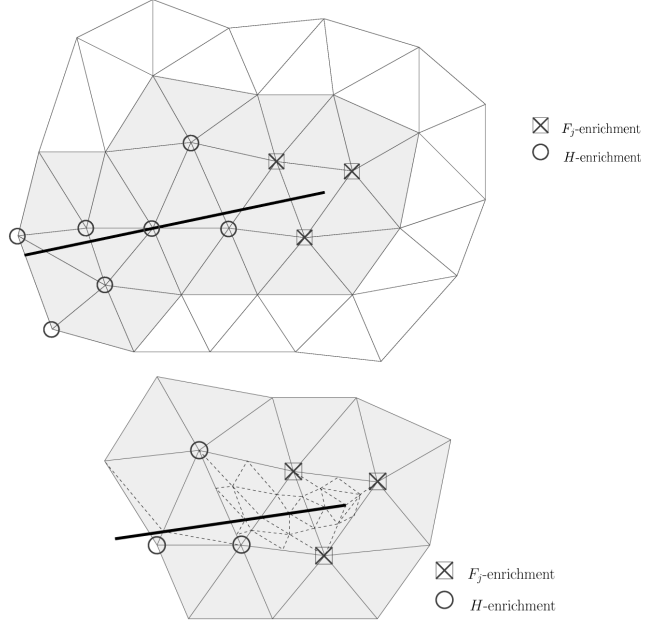


Fig. 3. Classical enrichment strategy and subdivision of the mesh for the purpose of numerical integration.

4 Representation of the discontinuity

As described in the previous section, the discontinuity of the displacement across the crack is taken into account in Xfem by the mean of an enrichment of the classical finite element space (defined on the uncracked domain) with a term of the form

$$\sum_{i \in I_H} b_i H \varphi_i,$$

where H is the step function, possibly defined via a function whose zero level set represents the geometry of the crack. It seems that this technique is the most optimal in Xfem. In [2] and [3], it is proven that the displacement is optimally approximated on each side of the crack. In our opinion, it is also one of the most original traits of Xfem. This technique can be extended to more complicated situations, for instance a situation where three zones instead of two are present, as it is illustrated in Fig. 4. This is already implemented and available in the Getfem library [11].

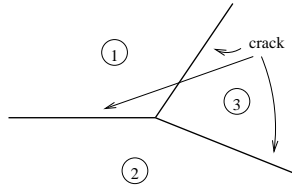


Fig. 4. A more complicated situation with three zones.

This technique can also be extended to take into account more complicated boundary conditions (for instance contact and friction condition, already treated in [5]). An important aspect to have an optimal approximation of the discontinuous part of the displacement is to use the same basis function in the enrichment as in the approximation of the displacement itself. Even when these basis functions does not represent a partition of unity (as it is the case for Hermite elements for instance). The fact that the Lagrange basis functions form a partition of unity is not the key point in that part of the enrichment.

5 Asymptotic displacement at the crack tip

In order to make a better approximation of the asymptotic displacement (and also the discontinuity) near the crack tip, a second enrichment of the form

$$\sum_{i \in I_F} \sum_{j=1}^4 c_{ij} F_j \psi_i,$$

is considered, where I_F is the set of basis function whose support contains the crack tip. Using this strategy, the convergence curve on Fig. 5 were obtained using the first opening mode u_I as the exact solution.

Some similar results can be found in [12]. The observed rate of convergence is limited to one half, even for high order methods like P_2 and P_3 . In the

following, we analyze this lack of accuracy and give some improvements for two-dimensional problems in order to recover a better convergence rate.

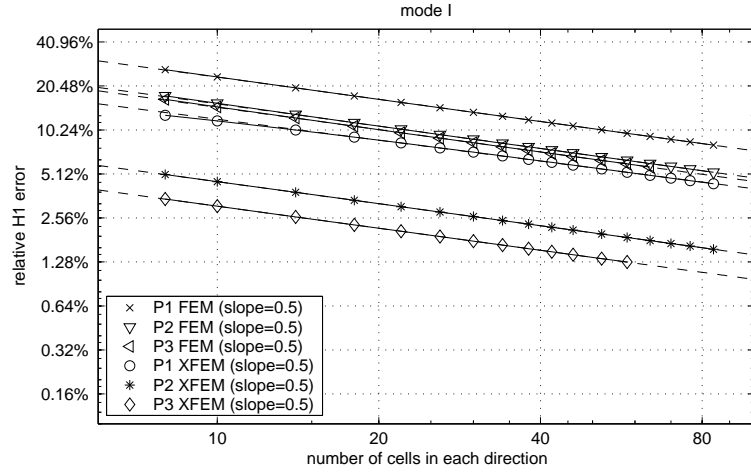
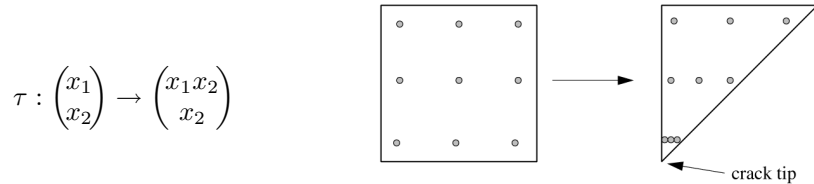


Fig. 5. Convergence curves for the classical Xfem and the first opening mode.

5.1 Adapted cubature formula for the asymptotic displacement



New integration points: $\bar{\xi} = \tau(\xi)$, new weights: $\bar{\eta} = \eta \det(\nabla \tau)$.

Fig. 6. The construction of adapted cubature formulas.

One of the difficulties which may degrade the quality of approximation is the fact that the gradients of the functions F_i , $i = 1..4$, are singular at the crack tip and the elementary integrals are not well approximated by classical cubature formulas. A remarkable aspect is that the singular part of the elementary integrals disappear when the computation is done in polar coordinates. Thus, we proposed in [7] the use of a simple adapted cubature formula on the sub-triangles having the crack tip as a vertex (see Fig. 3).

This adapted cubature formula is obtained from a classical Gauss formula on a square and using the transformation presented on Fig. 6. A convergence

test on the computation of an elementary matrix is presented on Fig. 7. Practically, with this method, 25 integration points were enough for the more accurate tests we done.

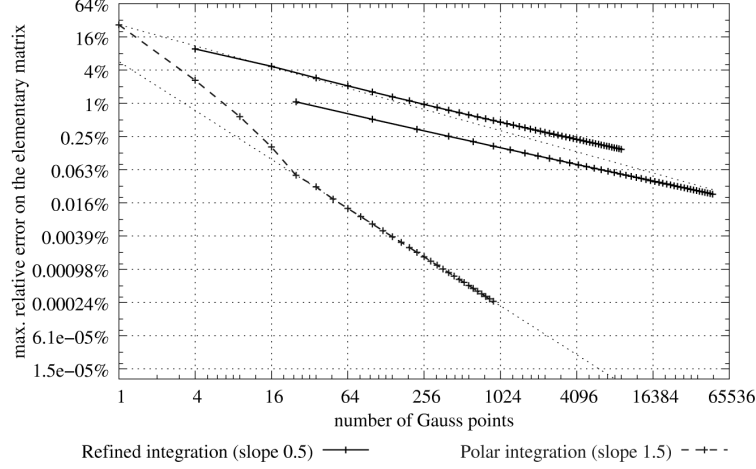


Fig. 7. Relative error on the computation of an elementary matrix with a refined order 3 Gauss method, a refined order 10 Gauss method and the almost polar method.

5.2 Fixed enriched area

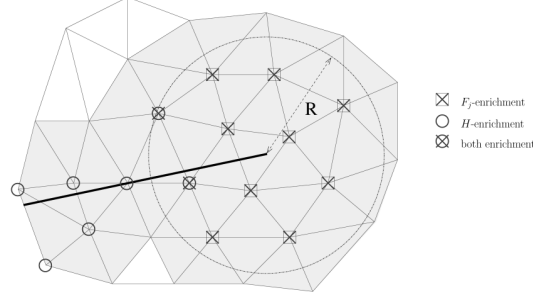


Fig. 8. Fixed enriched area method.

The second, and most important aspect which limits the convergence rate is the fact that the area enriched with the asymptotic displacement decreases with the mesh parameter h . A natural idea (independently proposed in [1]) is to have an enriched area independent of the mesh parameter. For instance, as it is presented on Fig. 8, all the nodes which are closer than a certain distance R (independant of h) will be enriched.

This gives the following enriched finite element space:

$$\mathcal{V}_R^h = \left\{ v^h = \sum_i a_i \varphi_i + \sum_{i \in I_H} b_i H \varphi_i + \sum_{i \in I_{F(R)}} \sum_{j=1}^4 c_{ij} F_j \psi_i : a_i, b_i, c_{ij} \in \mathbb{R}^2 \right\},$$

where $I_{F(R)}$ is the set of finite element nodes contained in the disk of radius R centered on the crack-tip. The convergence curves corresponding to this method are presented on Fig. 9. The convergence rates are close to be optimal.

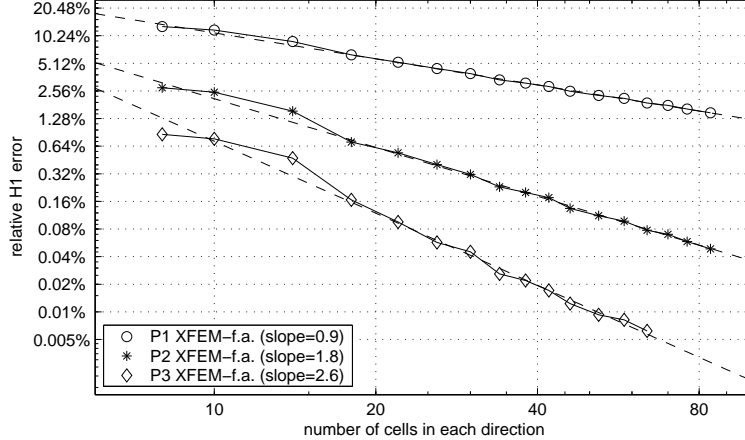


Fig. 9. Convergence curves of Xfem with a fixed enriched area.

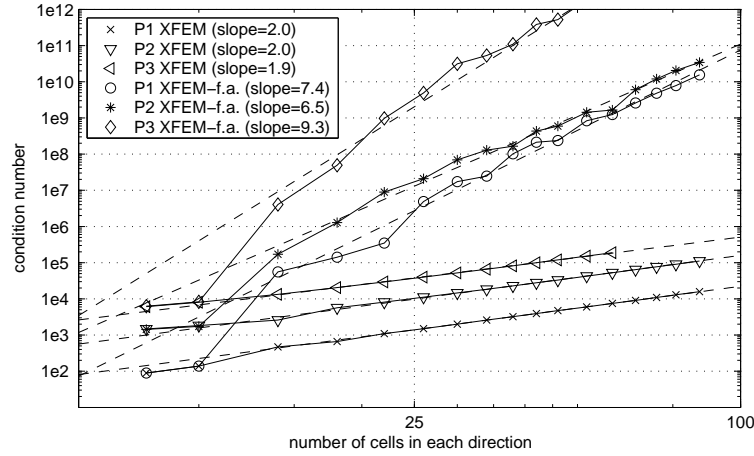


Fig. 10. Condition number of the linear system for Xfem with a fixed enriched area.

Unfortunately, as given on Fig. 10, the condition number of the linear system increases very rapidly when the mesh parameter decreases.

This is probably due to the fact that the basis functions of the enrichment are linearly dependent on an element (see [7]) and also to the fact that the functions $F_i, i = 1..4$ are somewhat flat far for the crack tip, and thus well approximated by the classical Fem.

6 Improvements for two-dimensional problems

In order to fix this difficulty, we present three techniques for two-dimensional problems:

- The dof gathering technique.
- Enrichment with the use of a cut-off function.
- Nonconforming method with a bonding condition.

All these methods are cheaper than Xfem with a fixed enriched area because the number of dof for the enrichment is very small. However, these techniques cannot be easily extended to three-dimensional problems.

6.1 The dof gathering technique

The dof gathering technique corresponds to prescribe the constraint

$$c_{ij} = c_{kj} \text{ for all } i, k \in I_{F(R)},$$

in the fixed enriched area method. This is equivalent to introducing

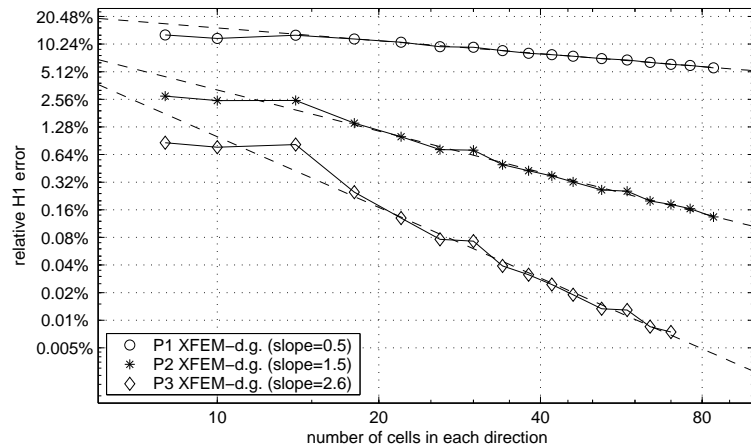


Fig. 11. Convergence curves for the dof gathering method.

$$T_R = \sum_{i \in I_{F(R)}} \psi_i,$$

and to considering the enrichment

$$\sum_{j=1}^4 c_j F_j T_R.$$

This reduces the number of enrichment dofs to only eight (four for each of the two components, see [7]). The convergence curves of this method are presented on Fig. 11.

One can see that half an order of convergence rate is lost. After analysis, this problem is due to the transition layer between the enriched area and the rest of the domain. However, the condition number of the linear system is greatly improved by this method (see Fig. 12).

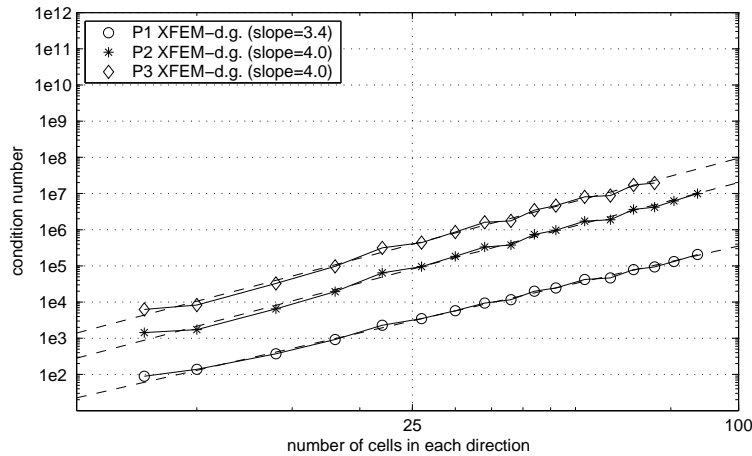


Fig. 12. Condition number of the linear system for the dof gathering method.

6.2 Enrichment with a cut-off function

Actually, the function $T_R = \sum_{i \in I_{F(R)}} \psi_i$ is a cut-off function which depends on the mesh parameter h and which is not regular. Instead of this function, the idea is to use a regular (\mathcal{C}^1 or \mathcal{C}^2) cut-off function γ which satisfies

$$\begin{cases} \gamma(r) = 1 & \text{if } r \leq r_0, \\ 0 < \gamma(r) < 1 & \text{if } r_0 < r < R, \\ \gamma(r) = 0 & \text{if } R \leq r. \end{cases}$$

where $0 < r_0 < R$. The enrichment is then defined by

$$\sum_{j=1}^4 c_j F_j \gamma.$$

The enrichment of a finite element space by the mean of a cut-off function was already presented in [13]. The complete numerical analysis of this method in the framework of Xfem is presented in [2] and [3]. The optimal convergence rate is obtained.

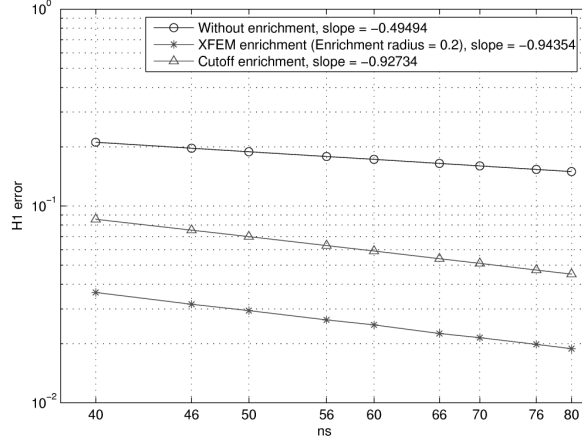


Fig. 13. Convergence curves for the cut-off method.

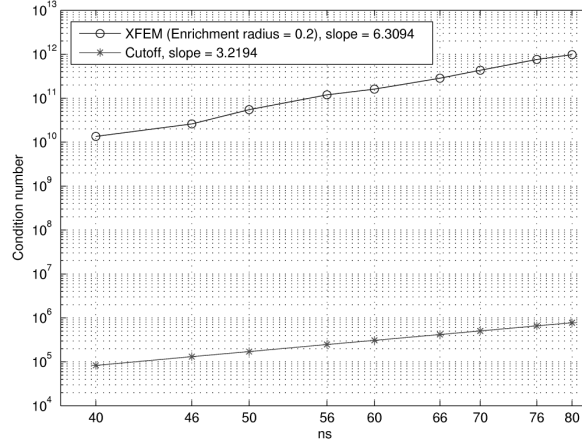


Fig. 14. Condition number of the linear system for the cut-off method.

This is illustrated on Fig. 13, where the enrichment with a cut-off function is compared to Xfem with a fixed enriched area. The optimal slope is close to be obtained. The fact that Xfem with a fixed enriched area gives a better approximation can be interpreted by the fact that the approximation is perturbated by the stiff part of the cut-off function in the present method. But, as presented on Fig. 14, the condition number is also greatly improved and the number of additional dofs is still only eight.

6.3 Enrichment with a bonding condition

Another technique, also presented in [7], is to simply enrich the finite element space by

$$\sum_{j=1}^4 c_j F_j.$$

but only on the elements contained in the enriched area. A pointwise bonding condition is then applied on the interface Γ_I between the enriched area and the rest of the domain on each finite element node (see Fig. 15).

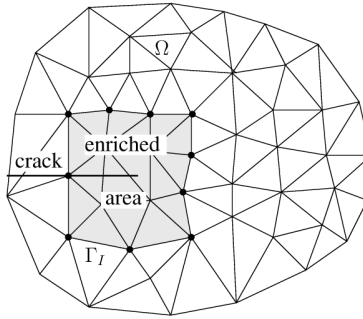


Fig. 15. Bonding condition method.

Numerically, this is the method the simplest to implement and one can see on Fig. 16 that this is also the most efficient. Fig. 17 represents a computation on a coarse mesh for the two opening modes with this technique and a P_3 method. The accuracy of the Von Mises stress is remarkable. In particular, the transition between the enriched area and the rest of the domain is not

visible.

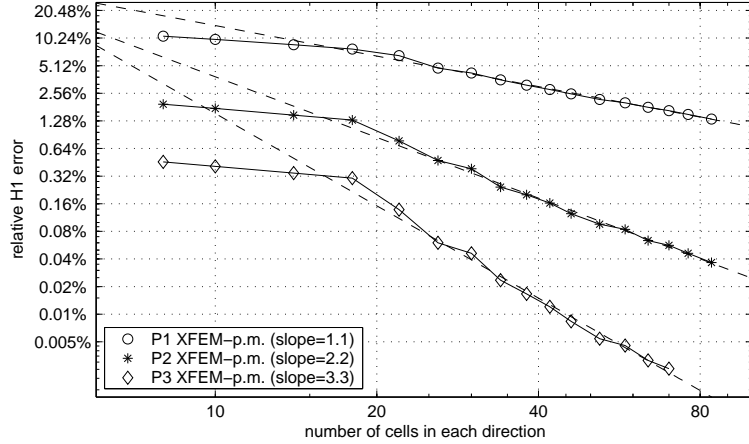


Fig. 16. Convergence curves for the enrichment with a bonding condition.

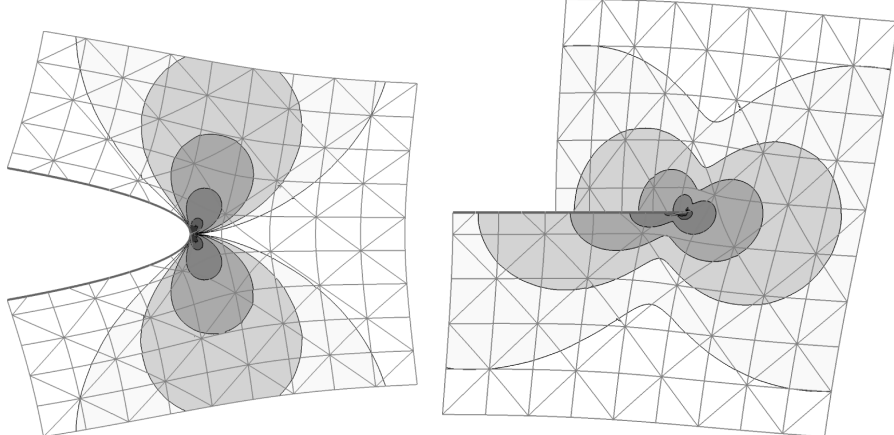


Fig. 17. P_3 XFEM solutions for the mode I and mode II problems with a pointwise bonding condition and a coarse mesh (contour levels of Von Mises stress).

Concluding remarks

In section 6 we propose three new techniques to improve Xfem method for two-dimensional domains. The extension of this work to three-dimensional problems is an open question, since the singularities are difficult to take into

account. Nevertheless the extension to plates and shells is more straightforward and is a work in progress.

References

1. E. Béchet, H. Minnebo, N. Moës and B. Burgardt. Improved implementation and robustness study of the X-FEM method for stress analysis around cracks. Submitted to *Int. J. Numer. Meth. Engng.*
2. E. Chahine, P. Laborde, Y. Renard. A quasi-optimal convergence result for fracture mechanics with XFEM. *C.R. Acad. Sci. Paris, Série I*, 342: 527–532, 2006.
3. E. Chahine, P. Laborde, Y. Renard. Crack-Tip enrichment in the Xfem method using a cut-off function. Submitted.
4. Ph. Destuynder, M. Djaoua. *Math. Meth. in the Appl. Sci.*, 3:70–87, 1981.
5. J. Dolbow, N. Moës, T. Belytschko. An extended finite element method for modeling crack growth with frictional contact. *Comput. Meth. Appl. Mech. Eng.*, 190: 6825–6846, 2001.
6. P. Grisvard. *Singularities in boundary value problems*. Masson, 1992.
7. P. Laborde, J. Pommier, Y. Renard, M. Salaün. High order extended finite element method for cracked domains. *Int. J. Numer. Meth. Engng.*, 64, 354–381, 2005.
8. J. Lemaître, J.-L. Chaboche *Mechanics of Solid Materials*. Cambridge University Press, 1994.
9. N. Moës, J. Dolbow, and T. Belytschko. A finite element method for crack growth without remeshing. *Int. J. Numer. Meth. Engng.*, 46:131–150, 1999.
10. N. Moës, A. Gravouil and T. Belytschko. Non-planar 3D crack growth by the extended finite element and level sets, Part I: Mechanical model. *Int. J. Numer. Meth. Engng.*, 53(11):2549–2568, 2002.
11. J. Pommier, Y. Renard Getfem++. *An open source generic C++ library for finite element methods*, <http://www-gmm.insa-toulouse.fr/getfem>.
12. F.L. Stazi, E. Budyn, J. Chessa, and T. Belytschko. An extended finite element method with higher-order elements for curved cracks. *Computational Mechanics*, 31:38–48, 2003.
13. G. Strang, G. J. Fix. *An Analysis of the Finite Element Method*. Prentice-Hall, Englewood Cliffs, 1973.
14. M. Stolarska, D.L. Chopp, N. Moës, T. Belytschko. Modelling crack growth by level sets in the extended finite element method. *Int. J. Numer. Meth. Engng.*, 51:943–960, 2001.